High-Efficiency InP-Based HEMT MMIC Power Amplifier for Q-Band Applications

W. Lam, M. Matloubian, A. Kurdoghlian, L. Larson, A. Igawa,
C. Chou, L. Jelloian, A. Brown, M. Thompson, and C. Ngo

Abstract— **Advanced millimeter-wave systems require high-efficiency MMIC power amplifiers to reduce physical size, weight, and prime power consumption. A high-efficiency MMIC power amplifier was developed using 0.15 um InP-based ($Al_{0.48}In_{0.52}As/Ga_{0.47}In_{0.53}As$) HEMT MMIC technology. The amplifier demonstrated state-of-the-art power performance, including 33% power-added efficiency and 24 dBm output power at 44 GHz. Potential applications include communication terminals and phased array antennas.**

I. Introduction

HIGH-EFFICIENCY MMIC power amplifier technology has been developing very rapidly in the last few years. This is due to the recent development of power HEMT and MESFET technology. Tserng *et al.* demonstrated a GaAs-based HEMT MMIC power amplifier with 40% power-added efficiency and 27-dBm output power at 30 GHz [1]. Kurdoghlian *et al.* developed a HEMT amplifier with 32% power-added efficiency and 27-dBm output power at 35 GHz [2]. Hegazi *et al.* demonstrated a MESFET amplifier with 15% power-added efficiency and 22.5-dBm output power at 43 GHz [3]. In this paper we will present the development of InP-based HEMT MMIC power amplifier. InP-based HEMT offers many advantages, including low noise figure, high gain, power added efficiency, current density, and thermal conductivity [4], [5].

II. Design

A large signal model of the HEMT device was developed to design the power amplifier on LIBRA. Figure 1 shows the model. The device had 6 gate fingers and 450-um gate width. The measured IV curve was fitted to the model. The initial values of the curve-fitting parameters were chosen from the measured IV characteristics (pinchoff voltage, saturated drain-to-source current, transconductance peak, and gate bias). The measured scattering parameter was also curve-fitted to the model at various bias conditions from 1 to 60 GHz. The parasitic elements were determined using the data taken from the cold bias condition. Consequently, the curve-fitting process was quite fast and accurate. The source impedance for high gain performance and load impedance for high power and efficiency were simulated to design the matching networks. The simulated source impedance was $5 + j2.5$ ohms and the load impedance was $17.5 + j1.8$ ohms at 44 GHz.

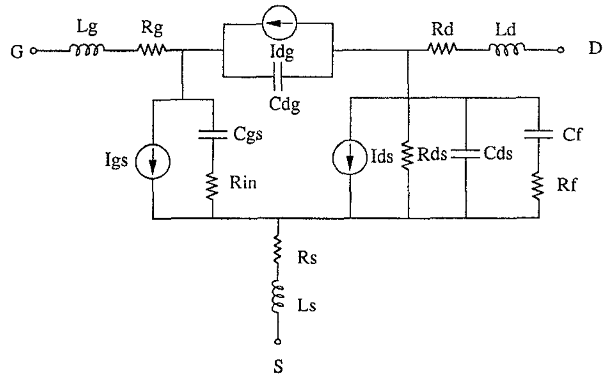

Fig. 1. Large signal model of InP-based HEMT.

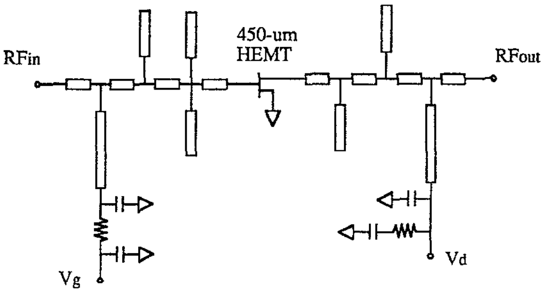

Fig. 2. Power amplifier design.

The design was a single-stage amplifier suitable for driver development. Figure 2 shows the equivalent circuit. The input and output matching networks utilized double tuning stubs to match the low impedance of the device to 50 ohm over wide frequency. The bias networks employed lump-element resistors and capacitors to stabilize the amplifier in the out-of-band frequency. The chip dimensions were 1.9×2 mm^2. The simulated power added efficiency was 31%, and output power was 23 dBm at 44 GHz.

III. Fabrication

The fabrication began with material growth. Figure 3 shows the epitaxial structure. The average sheet resistance was about 200 ohm per square, and electron carrier concentration was about 4×10^{12} cm^{-2}. AuGe/Ni/Au ohmic contacts were

Manuscript received July 6, 1993. This work was sponsored by MILSTAR System Program Office (ESD/MS), Electronic Systems Division, Hanscom Air Force Base, Bedford, MA 01731.

W. Lam, A. Kurdoghlian, and A. Igawa are with Hughes Microelectronic Circuits Division, Torrance, CA 90509.

M. Matloubian, L. Larson, C. Chou, L. Jelloian, A. Brown, M. Thompson, and C. Ngo are with Hughes Research Laboratory, Malibu, CA 90265.

IEEE Log Number 9213206.

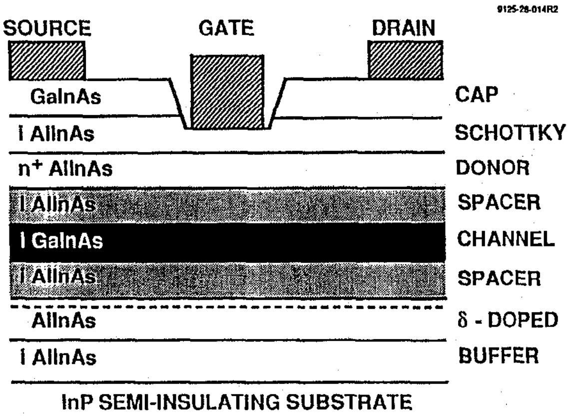

Fig. 3. HEMT cross section.

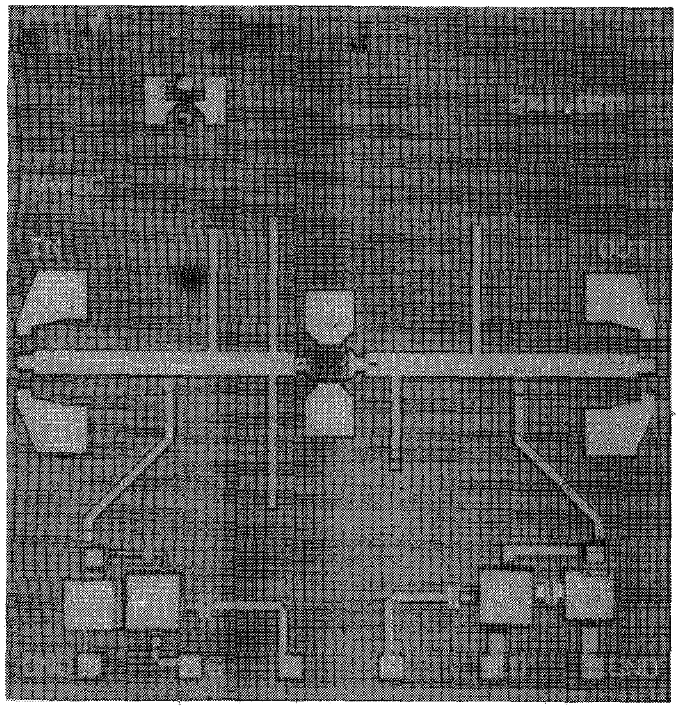

Fig. 4. Q-band MMIC power amplifier.

formed next. The contact resistance was typically less than 0.15 ohm-mm. Boron was implanted at multiple acceleration voltages to isolate the active devices. The probe-to-probe resistance was typically greater than 1 mega ohm. The gate-length was 0.15 um defined by a Phillips beam writer. Next Ti/Pt/Au was deposited and lifted off to form the gate. The gate resistance was typically 200 ohm/mm. Subsequently first-level metallization was deposited to overlay the device terminals and print the transmission lines. The active device was passivated with silicon nitride and metal-insulator-metal capacitors were developed using silicon oxide. The capacitance density was approximately 240 pF/mm^2. Then airbridges were fabricated and metallization of transmission lines was gold plated to handle more than 15 mA/um current density. Next the wafer was thinned to 4-mil thickness. Via holes were etched and gold plated to provide low inductance RF ground. Finally the wafer was scribed and broken into individual chips. Figure 4 shows the fabricated MMIC power amplifier.

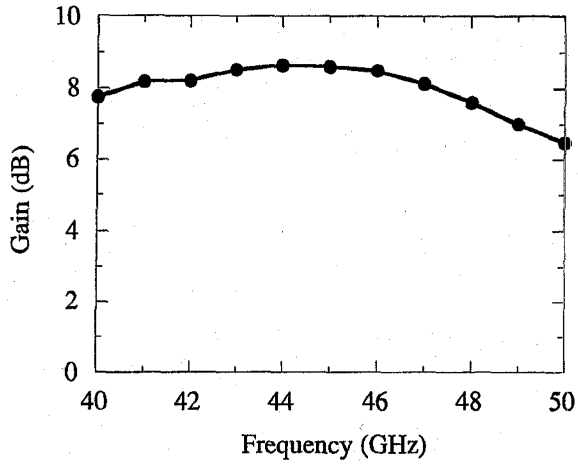

Fig. 5. Measured small signal gain.

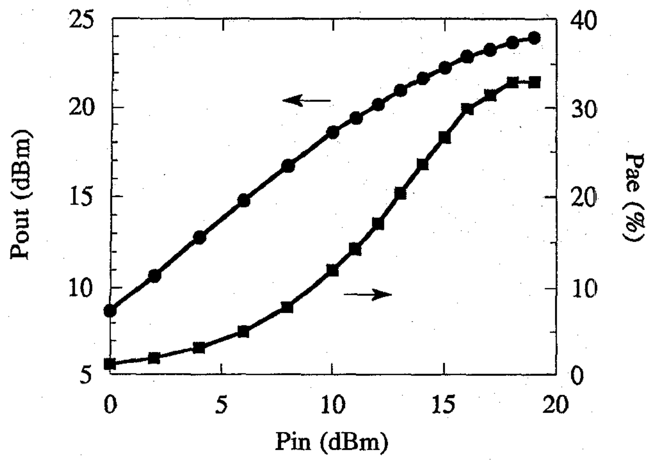

Fig. 6. Measured output power and efficiency.

IV. Result

The small signal performance of the amplifier was measured on wafer using Cascade Microtech probes and the Wiltron network analyzer. The measurement system was calibrated with the through-reflect-match technique. Figure 5 shows the measured gain response. The small signal gain was 8.6 dB at 44.5 GHz. The gain variation was less than 0.2 dB from 43 GHz to 46 GHz. The power performance of the amplifier was measured on test fixture using E-plane probe transitions. The measured insertion loss of the test fixture was 1.4 dB at 44 GHz, which was used to de-embed the performance of the amplifier. Figure 6 shows the measured output power and power-added efficiency. The maximum power-added efficiency was 33%, and the associated output power and gain were 24 dBm and 5 dB, respectively. The linear gain was 8.5 dB, which agrees well with the measured small signal gain on wafer. Figure 7 shows the measured gain and compression characteristics. The gain varied less than 0.2 dB under small signal condition. The 1-dB compression point occurred at about 14 dBm input power. The corresponding output power and efficiency were 21.6 dBm and 23%, respectively.

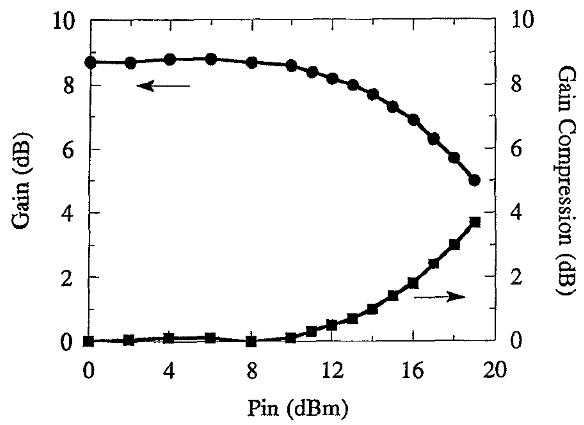

Fig. 7. Measured gain and compression characteristic.

V. Conclusion

A high-efficiency Q-band InP-based HEMT MMIC power amplifier was developed and demonstrated state-of-the-art power performances in one design iteration. The amplifier exhibited 33% power-added efficiency, 24-dBm output power, 5-dB associated power gain, and 8.5-dB linear gain at 44 GHz. The gain flatness is better than 0.2 dB in the MILSTAR frequency band. These results show that InP-based HEMT MMIC power amplifier is a new and promising technology for advanced millimeter-wave system applications.

Acknowledgment

The authors would like to thank R. Lohr for layout support, S. Rosenbaum for device measurement assistance, D. Pierson for MMIC post process, Huy Nghiem for MMIC evaluation, and J. Chen and R. Ying for technical suggestions. We would also like to thank the MILSTAR System Program Office, Hanscom, for their foresight and encouragement in sponsoring the development.

References

[1] H. Q. Tserng, P. Saunier, and Y. C. Kao, "High-efficiency broadband monolithic pseudomorphic HEMT amplifier at Ka band," *IEEE Microwave and Millimeter-Wave Monolithic Circ. Symp. Digest*, pp. 51–54, 1992.

[2] A. Kurdoghlian *et al.*, "The demonstration of Ka-band multi-functional MMIC circuits fabricated on the same PHEMT wafer with superior performance," to be published in *IEEE Microwave Theory and Technique Symp. Digest*, 1993.

[3] G. Hegazi *et al.*, "GaAs molecular beam epitaxy monolithic power amplifiers at U band," *IEEE Microwave and Millimeter-Wave Monolithic Circ. Symp. Digest*, pp. 121–125, 1989.

[4] U. K. Mishra and A. S. Brown, "InGaAs/AlInAs HEMT technology for millimeter wave applications," *IEEE GaAs IC Symp. Digest*, pp. 97–99, 1988.

[5] M. Matloubian *et al.*, "V-band high-efficiency high-power AlInAs/GaInAs/InP HEMTs," *IEEE Microwave Theory and Technique Symp. Digest*, pp. 535–537, 1993.